Journal of Ceramic Processing Research. Vol. 9, No. 1, pp. 13~18 (2008)

J O U R N A L O F
Ceramic
Processing Research

Effects of aging on the phase transformation and sintering properties of coprecipitated Al_2O_3-ZrO_2 powders

Chih-Cheng Chen[a,b], Hsing-I Hsiang[b,*] and Fu-Su Yen[b]

[a]*Department of Mechanical Engineering, Far EastCollege, Tainan, Taiwan, R.O.C.*

[b]*Particulate Materials Research Center, Department of Resources Engineering, National Cheng Kung University, Tainan, Taiwan, R.O.C.*

In this study, the effects of aging on the crystalline phases, crystallite sizes and sintering properties of coprecipitated Al_2O_3-ZrO_2 powders are investigated using thermogravimetry (TG), differential thermal analysis (DTA), X-ray diffractometry (XRD), dilatometry, scanning electron microscopy (SEM) and transmission electron microscopy (TEM). Coprecipitated Al_2O_3-ZrO_2 powder aging in the solution promoted the dissolution and reprecipitation process, which resulted in the boehmite structure subsequently transforming into bayerite. The densification and microstructural development of the coprecipitated Al_2O_3-ZrO_2 powders were dependent upon the aging time which shifted the $\theta \rightarrow \alpha$-$Al_2O_3$ phase transformation to a higher temperature, lowered the crystallite growth rate, and prevented the occurrence of intragranular ZrO_2 particles during sintering.

Key words: Ceramics, coprecipitation, Al_2O_3-ZrO_2, Phase transformation, Sintering

Introduction

An alumina-zirconia composite can be used as a structural ceramic with excellent mechanical properties [1-3]. Zirconia-toughened alumina (ZTA) toughening has been attributed to stress-induced transformation or micro-crack nucleation [4]. Maintaining zirconia in the tetragonal phase is essential for stress-induced transformation toughening, whereas a uniform zirconia particle distribution is important for optimizing micro-crack nucleation-induced toughening [3]. The dispersed zirconia particles must be smaller than a critical size to retain the tetragonal phase [4]. This requires certain special techniques, especially when a uniform zirconia particle distribution in the alumina matrix is also desired. Hence, many wet chemical methods have been used to control the alumina-zirconia composite microstructure, such as spray pyrolysis [5], sol-gel [6], and evaporative decomposition methods [7]. The coprecipitation method is attractive for large-scale powder production because of the homogeneous mixing on the atomic scale [8].

Aging is a process by which the physical properties of the precipitates can change as a result of the following mechanisms: polymerization, coarsening, and a phase transformation [9]. The changes in the precipitate structure and properties that occur during aging have a profound effect on the subsequent sintering process [10]. Various studies have shown that amorphous alumina and zirconia gels could be converted into crystalline products using an aging process [11-12]. These reports have focused mainly on the aging effects on the crystallization, specific surface area, and crystallite size of the precipitates. However the mechanisms of the effects of aging treatment on the crystallization, phase transformation, and sintering properties of the coprecipitated Al_2O_3-ZrO_2 powders have not been well understood.

The aim of this study is to use a coprecipitation method to prepare Al_2O_3-ZrO_2 powders and investigate the aging effects on the crystalline phases, phase transformation, and sintering properties of the coprecipitated Al_2O_3-ZrO_2 powders using TG, DTA, XRD, dilatometry, SEM and TEM.

Experimental

Sample preparation

$Al(NO_3)_3 \cdot 9H_2O$ (Ishizu Pharmaceutical Co. Ltd., Japan) and $ZrO(NO_3)_2 \cdot 2H_2O$ were dissolved in distilled water to prepare the starting solution. The precipitates were prepared by adding NH_4OH solution into the mixed starting solution to achieve pH 9.0 under vigorous stirring. The Al_2O_3-ZrO_2 powders were prepared at a ratio of 85 Al_2O_3/15 ZrO_2 vol%. After precipitation, the precipitates were aged in the same containers for 0.5, 6, 12, 24, 40 h, separately (sample A0.5, A6, A12, A24, A40). After aging, distilled water was used for filtering and washing three times. The precipitate was then washed with ethanol and dried at 80°C. All samples were calcined at 900°C for 1 h and then ground to less than 200 mesh

*Corresponding author:
Tel : +886-6-2757575ext 62821
Fax:886-6-2380421
E-mail: hsingi@mail.ncku.edu.tw

size. Green compacts were prepared using a cylindrical die, 1.2 cm in diameter, under a 500 MPa pressure. Powders were sintered at 1550°C (heating rate 10 K minute^{-1}) for 4 h.

Characterization

The crystalline phase and chemical composition of the calcined specimens were characterized using an X-ray diffractometer with Cu-K_α(Rigaku, D/MAX IIB) and an FTIR spectrometer (Bruker EQUINOX 55), respectively. The XRD powder method was also employed to determine the quantities of crystallized zirconia by adding 10wt% CaF_2 as the internal standard. The specific surface areas of the specimens were determined using a surface area analyzer (Micromeritics 2200). The thermal shrinkage measurements (Netzsch DIL 420C) and DTA/TG (Netzsch STA 409C) analyses were performed using alumina as the reference material. The microstructural development of the sintered pellet was observed by TEM (Hitachi 700H) and SEM (Joel JSM-35F).

Results and discussion

Effects of aging on the thermal behavior and phase development of the coprecipitated Al_2O_3-ZrO_2 powders

Table 1 shows XRD results for the coprecipitated Al_2O_3-ZrO_2 powders aged for various durations. The coprecipitated Al_2O_3-ZrO_2 powder aged for 0.5 h was a mixture of pseudoboehmite and amorphous ZrO_2. For the coprecipitated Al_2O_3-ZrO_2 powders aged for 6, 12, 24, and 40 h, pseudoboehmite and bayerite peaks were observed. The FTIR spectra of the coprecipitated Al_2O_3-ZrO_2 powders aged for various durations are shown in Fig. 1. For the samples aged for 0.5 and 6 h, an absorption band at about 2400 cm^{-1} attributed to the characteristic absorption peak of pseudoboehmite [14] was observed. The absorption bands at 760, 630 and 500 cm^{1} related to the Al-O stretching vibration and 1143 cm^{1} associated with the O-H stretching vibration of the boehmite [15] were also observed. In the case of the samples aged for 24 and 40 h, absorption bands at about 976, 1016 cm^{-1} and 3600 cm^{-1} attributed to the OH bending and stretching of bayerite [16-17] were observed.

Figure 2 shows the changes in the DTA/TG profiles for the coprecipitated Al_2O_3-ZrO_2 powders with various aging times. Three peaks are observed in the samples aged for 0.5 and 6 h at around 170, 450, and 1300°C.

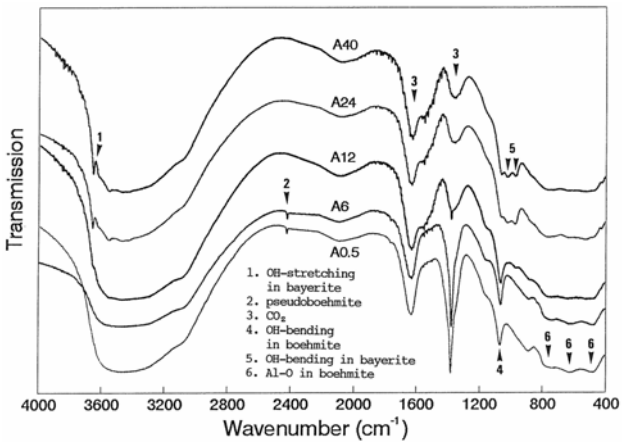

Fig. 1. FTIR spectra of the coprecipitated Al_2O_3-ZrO_2 powders aged for various durations.

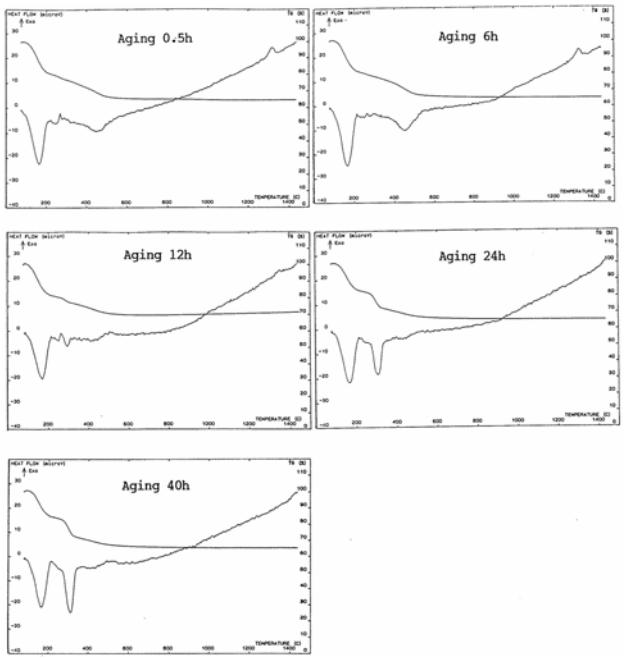

Fig. 2. DTA/TG profiles for the coprecipitated Al_2O_3-ZrO_2 powders with various aging times.

The first endothermic peak (170°C) is attributed to the desorption of water molecules. The second endothermic peak (450°C) may correspond to the pseudoboehmite → r-Al_2O_3 phase transformation. The third exotherm (1300°C) is attributed to the θ → α-Al_2O_3 phase trans-

Table 1. XRD results for the coprecipitated Al_2O_3-ZrO_2 powders aged for various durations.

Aging time (h)	Dried gel	Calcined powders (900°C, 1h)	Calcined powders (1200°C, 1h)	Calcined powders (1300°C, 1h)
0.5	P, A	(δ), (θ), t	θ, t	α, (θ), t
6	P, (B), A	(δ), (θ), t	θ, t	α, (θ), t
12	P, B, A	δ, θ, t	θ, t	α, θ, t
24	P, B, A	(δ), θ, t	θ, t	(α), θ, t
40	P, B, A	(δ), θ, t	θ, t	(α), θ, t

P: pseudoboehmite; A:amorphous ZrO_2; B: bayerite; δ: δ-Al_2O_3; θ: θ-Al_2O_3; t: t-ZrO_2; α: α- Al_2O_3; m: m-ZrO_2; ( ): weak

formation. For the samples aged above 12 h, the peaks attributed to the pseudoboehmite → r-Al_2O_3 and θ → α-Al_2O_3 phase transformations disappeared. However, a new endothermic peak around 300°C due to the bayerite → η-Al_2O_3 phase transformation and a new exothermic peak around 500°C due to the crystallization of tetragonal zirconia were observed. These results are consistent with the previous observations [12-13] and suggest that aging the coprecipitated Al_2O_3-ZrO_2 powders in the solution promoted the dissolution and reprecipitation process, which resulted in the boehmite subsequently transforming into bayerite.

Srdic and Radonjic [18] prepared alumina-zirconia composites using a sol-gel process and observed that a mutual interaction existed between the zirconia and the transitional aluminas, which affected the phase transformation and microstructural development of the alumina matrix, if the alumina and zirconia particles are smaller and more intimately mixed. The Al_2O_3-ZrO_2 powder prepared using coprecipitation possesses a homogeneous mixing on the atomic scale, which leads to an intimate interaction between the alumina and zirconia. However, aging after coprecipitation can result in physical and chemical changes due to the following mechanisms: [19] (a) recrystallization of primary particles into more compact shapes through surface diffusion or mass transport through the liquid phase; (b) transformation of metastable modifications into stable modifications by dissolution and recrystallization. The as-coprecipitated Al_2O_3-ZrO_2 powder was the least stable supersaturated Al_2O_3-ZrO_2 solid solution. The as-coprecipitated Al_2O_3-ZrO_2 powder could then reduce its free energy by phase partitioning, which may occur into mixtures with different phases by dissolution and reprecipitation during aging and weaken the interaction between the alumina and zirconia.

Figure 3 shows the XRD patterns of the coprecipitated Al_2O_3-ZrO_2 powders with various aging times calcined at 1200°C. It shows that all samples were a mixture of θ-Al_2O_3, tetragonal (t-) and monoclinic (m-) zirconia. The amount of crystallized zirconia for the samples with various sintering times at 1200°C was semiquantitatively determined by calculating the ratio of the integrated intensities of the (111) peak of tetragonal zirconia and the (111) peak of monoclinic zirconia to that of the (111) peak of the internal standard (CaF_2). The results are shown in Fig. 4 and indicate the intensity of t- and m-ZrO_2 in the samples calcined at 1200°C increased with increasing aging time. This may be due to coprecipitated Al_2O_3-ZrO_2 powders with shorter aging time possessing a stronger interaction between the alumina and zirconia, which enhances more zirconia incorporation into the θ-Al_2O_3. Figure 5 shows the XRD patterns of the coprecipitated Al_2O_3-ZrO_2 powders with

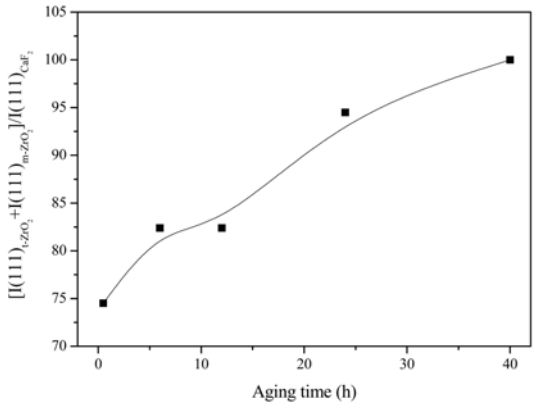

Fig. 4. Integrated intensities of the (111) peak of tetragonal zirconia and the (111) peak of monoclinic zirconia to that of the (111) peak of the internal standard (CaF_2).

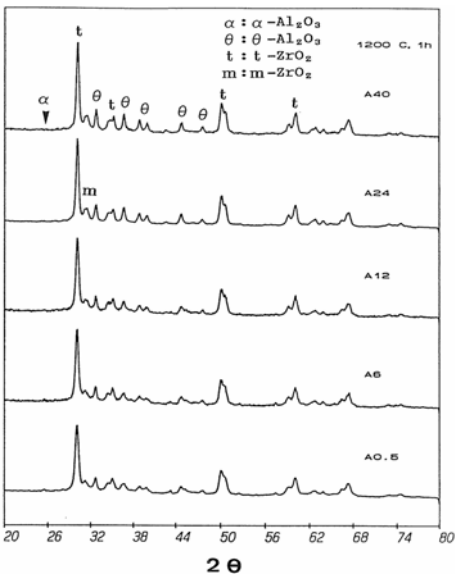

Fig. 3. XRD patterns of the coprecipitated Al_2O_3-ZrO_2 powders with various aging times calcined at 1200°C.

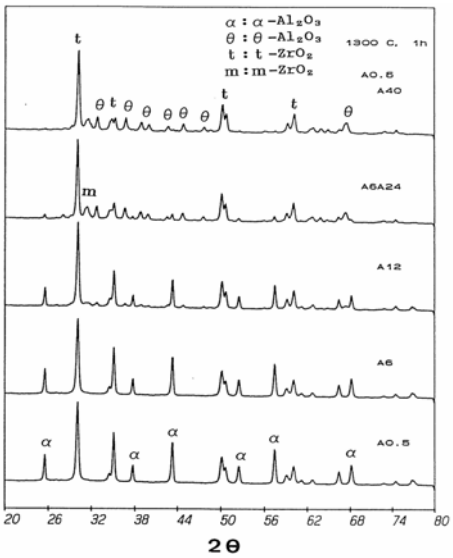

Fig. 5. XRD patterns of the coprecipitated Al_2O_3-ZrO_2 powders with various aging times calcined at 1300°C.

various aging times calcined at 1300°C. The intensity of the α-Al_2O_3 phase decreased with increasing aging time, indicating that the aging process could retard the transformation into α-Al_2O_3. The $\theta \rightarrow \alpha$ phase transformation of nano-sized Al_2O_3 powder is performed by a nucleation and growth process. The interface between two contacting α-Al_2O_3 particles can provide the sites for nucleation of the θ-Al_2O_3 phase. Thus the nucleation rate is determined by the probability of contact between two θ-Al_2O_3 particles. Wen and Yen [20] studied the $\theta \rightarrow \alpha$-$Al_2O_3$ phase transformation and discovered that only after θ-Al_2O_3 coarsens to a critical size (~20 nm) can it start to transform into α-Al_2O_3. Generally speaking, crystallite growth in nanocrystallites can be regarded as the coalescence of small neighboring crystallites due to atomic diffusion or discrete orientation attachment of crystallographically oriented crystallites [21]. The interface between two contacting θ-Al_2O_3 particles can provide the sites for nucleation of the α-Al_2O_3 phase. Thus the nucleation rate is determined by the probability of contact between two θ-Al_2O_3 particles. The amount of crystallized zirconia increased with increasing aging time, indicating that aging promoted more Zr^{+4} ions to become expelled from the lattice of transitional alumina and precipitate as zirconia particles (Fig.4). Because the precipitated zirconia particles can prevent θ-Al_2O_3 particles from coming into contact, this suppresses the coalescence of θ-Al_2O_3 particles to retard the $\theta \rightarrow \alpha$-$Al_2O_3$ phase transformation.

As the calcination temperature increased to 1300°C, the intensity of t- and m-ZrO_2 for samples aged for various times became nearly the same. This may be attributed to the expulsion of zirconia dissolved in θ-Al_2O_3 occurring for the sample aged for a shorter time because of the lower zirconia solubility in the α-Al_2O_3.

Effects of aging on the shrinkage behaviors and microstructural development

The shrinkage curves of coprecipitated Al_2O_3-ZrO_2 powders for various aging times are demonstrated in Fig. 6. The shrinkage could be divided into three stages according to the $\theta \rightarrow \alpha$-$Al_2O_3$ phase transformation as shown below:

(1) Stage I (the temperature range between the shrinkage onset temperature and that of the $\theta \rightarrow \alpha$-$Al_2O_3$ phase transformation): The sintering of the θ-Al_2O_3 was dominated during stage I. The samples aged for 0.5 and 6 h experienced a faster crystallite growth to the critical size of the $\theta \rightarrow \alpha$-$Al_2O_3$ phase transformation at 1300°C. The $\theta \rightarrow \alpha$-$Al_2O_3$ phase transformation for the samples aged for 0.5 and 6 h occurred at above 1300°C, at which the linear shrinkage were about 21% and 20%, respectively. For the samples aged at 12, 24 and 40 h, the $\theta \rightarrow \alpha$-$Al_2O_3$ phase transformation was shifted to about 1370°C due to the precipitated zirconia particles which suppressed the coalescence of θ-Al_2O_3 particles, which inhibited the $\theta \rightarrow \alpha$-$Al_2O_3$ phase transformation and the linear shrinkages were about 10, 12.8 and 17.8%, respectively. Note that the densification rate and linear shrinkage for the stage I decreased with increasing aging time. This may be due to samples aged for shorter times having a higher surface area (Fig. 7), which resulted in a higher sintering driving force and linear shrinkage.

At this stage, the linear shrinkage was dependent on

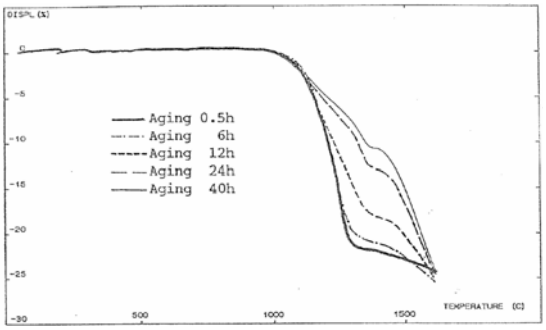

Fig. 6. Shrinkage curves of coprecipitated Al_2O_3-ZrO_2 powders for various aging times.

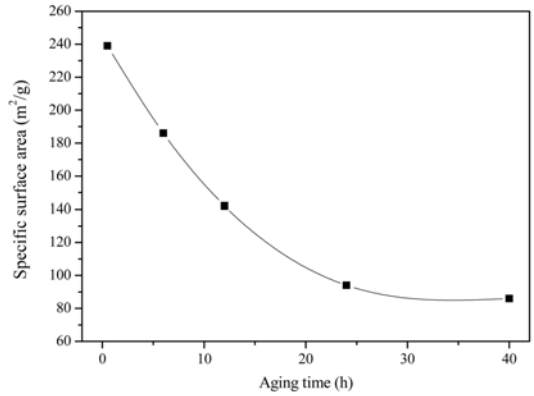

Fig. 7. Change in the specific surface area of coprecipitated Al_2O_3-ZrO_2 powders with various aging times.

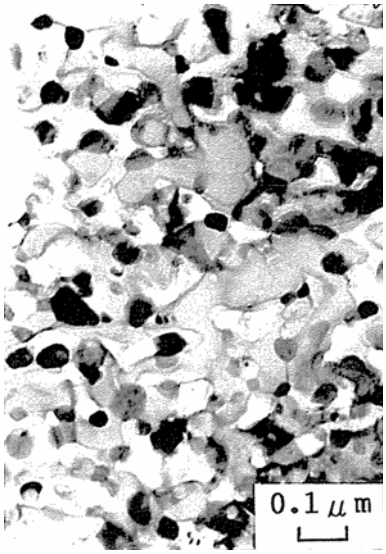

Fig. 8. Transmission electron micrographs of the sample with aging time of 0.5 h sintered at 1350°C for 5 minutes.

the θ-Al_2O_3 crystallite sizes and the onset temperatures of the θ → α-Al_2O_3 phase transformation.

(2) Stage II (temperature range of θ → α-Al_2O_3 phase transformation): During the θ → α-Al_2O_3 phase transformation, the coalescence of crystallites and necking were developed, which retarded densification as well as shrinkage. Therefore, the rate of shrinkage slowed down at stage II, as shown in Fig.6. For the sample aged for 0.5 h, the θ→α-Al_2O_3 phase transformation occurred at around 1300°C and large pores, very fine particles of t-ZrO_2 included within the coarse α-Al_2O_3 grains found in the sample aged for 0.5 h were attributed to the development of a coarse, vermicular pore structure during transformation to α- Al_2O_3 as shown in Fig. 8. For the samples with aging times of 12 and 24 h, the region of phase transformation was shifted to 1370°C. The temperature range of stage II of a sample decreased with increasing aging time.

(3) Stage III (the temperature range of the stage was between the offset temperature of the θ → α\-Al_2O_3 phase transformation and the final densification temperature): The densification rate of the stage was affected by the microstructure after the θ→α-Al_2O_3 phase transformation. For the samples aged for 0.5 and 6 h, crystallite coalescence accompanied with the θ → α-Al_2O_3 phase transformation inhibited further densification (Fig. 6). However, for samples with an aging time above 12 h, crystallite growth of α-Al_2O_3 was suppressed due to the pinning effect of intergranular ZrO_2 after the θ→α-Al_2O_3 phase transformation, which resulted in a better densification rate than samples with aging times of 0.5 and 6 h.

Figure 9 shows the microstructural development of the coprecipitated Al_2O_3-ZrO_2 powders with various aging times sintered at 1550°C. In the case of the samples with aging times above 12 h, the ZrO_2 particles remain mainly at the grain boundaries and cannot be observed within the alumina matrix grains. However, the inclusion of zirconia particles and pores within the α-alumina grains occurred in the samples aged for 0.5 and 2 h during the θ to α transformation. The smaller ZrO_2 particles seem to be entrapped within the alumina grains and the larger ZrO_2 particles seem to remain at the grain boundaries. Stough and Hellmann [22] investigated the solid solubility of zirconia in α-Al_2O_3 and observed that a zirconia solubility of 0.004-0.027wt% and that tetragonal zirconia (~10 nm) precipitated from supersaturated α-Al_2O_3 and became entrapped within the alumina matrix. Pugar and Morgan [23] also reported that the development of fine-grained ZrO_2 within the α-Al_2O_3 is associated with the θ → α-Al_2O_3 phase transformation. Therefore, for the samples with aging times of 0.5 and 2 h sintered at 1300°C, the£c-Al_2O_3 transformed to θ-Al_2O_3 and partitioning phases occurred due to the lower solubility of zirconia in the α-Al_2O_3 than in transition Al_2O_3, which led to the precipitation of very fine particles of t-ZrO_2 (less than 50 nm) within the α-Al_2O_3 matrix (Fig.9).

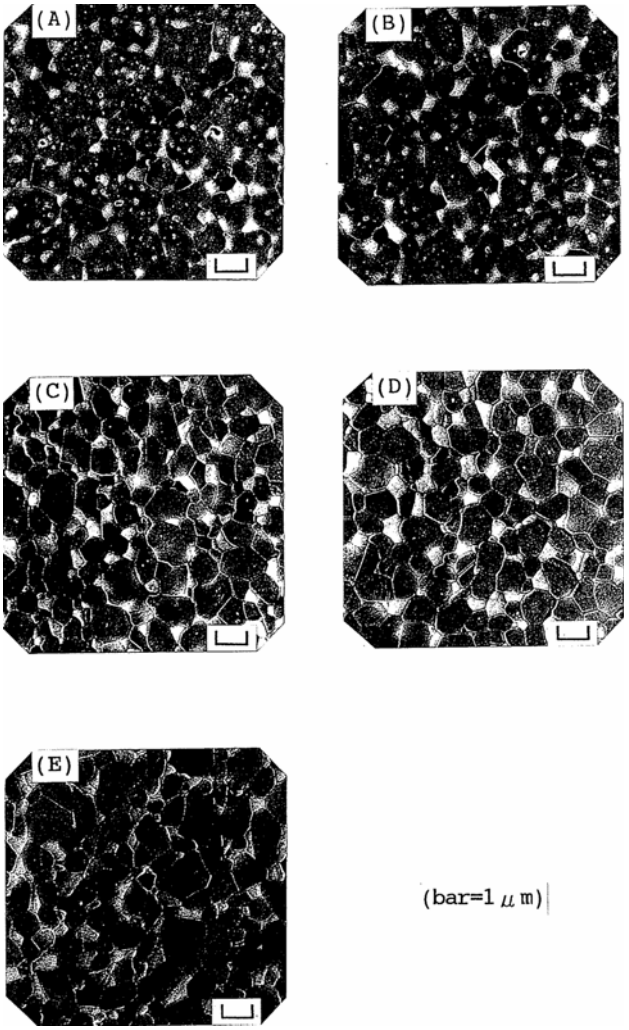

Fig. 9. Scanning electron micrographs of the coprecipitated Al_2O_3-ZrO_2 powders with various aging times sintered at 1550°C (A) A0.5, (B) A6, (C) A12, (D) A24, (E) A40.

Conclusions

(1) The aging of coprecipitated Al_2O_3-ZrO_2 powders in a solution evidently promoted the dissolution and reprecipitation process, which resulted in the boehmite subsequently transforming into bayerite.

(2) The densification and microstructural development of the coprecipitated Al_2O_3-ZrO_2 powders were dependent upon the aging time which shifted the θ → α-Al_2O_3 phase transformation to a higher temperature, lowered the crystallite growth rate, and prevented the occurrence of intragranular ZrO_2 particles during sintering.

Acknowledgement

The authors would like to express their thanks to the National Science Council of the Republic of China (NSC94-2622-E-006-011-CC3) and the Ministry of Economic Affairs (92-EC-17-A-08-S1-023) through the Particulate Materials Research Center of National Cheng Kung University for financially supporting this project.

References

1. N. Claussen, J. Am. Ceram. Soc., 59 [1–2] (1976) 49-51.
2. F. F. Lange, J. Mater. Sci., 17 (1982) 225-62.
3. S. Hori, M. Yoshimura, and S. Somiya, J. Am. Ceram.Soc., 69 [3] (1986) 169-72.
4. A. H. Heur, N. Claussen, W. M. Kriven, M. Ruhle, J. Am. Ceram. Soc., 65 [12] (1982) 643-50.
5. A. S. Gandhi, V. Jayaram, A. H. Chokshi, J. Am. Ceram. Soc., 82 [10] (1999) 2613-18.
6. J. Kuo, D. L. Bourell, J. Mater. Sci., 32 (1997) 2687-92.
7. D. W. Sproson, G. L. Messing, J. Am. Ceram. Soc., 67 [5] (1984) C92-93.
8. J. Wang, R. Raj, J. Am. Ceram. Soc., 74 [7] (1991)1707-709.
9. C. J. Brinker, G. W. Scherer, in "Sol-gel science: The physics and chemistry of sol-gel processing" (Academic Press, Inc., San Diego, 1990) p.357-405.
10. H. I. Hsiang, S. C. Lin, Mater. Chem. Phys., 95 [2-3] (2006) 275-279.
11. H. I. Hsiang,S. C. Lin, Mater. Sci. Eng. A, 380 [1-2] (2004) 67-72.
12. J. M. Rousseaux, P. Weisbecker, H. Muhr, E. Plasari, Ind. Eng. Chem. Res., 41 (2002)6059-69.
13. P. Jakubus, A. Adamski, M.Kurzawa, Z. Sojka, J. Therm. Anal. Cal., 72 [1] (2003) 299-310.
14. J. J. Fripiat, H. Bosmans, P.G. Rouxhet, J. Phy. Chem., 71 [4] (1967) 1097-11.
15. I. H. Joe, A. K. Vasudevan, G. Aruldhas, A. D. Damodaran, K. G.. K. Warrier, J. Solid State Chem. 131 (1997) 181-184.
16. H. Wijnja, C. P. Schulthess, Spectrochim. Acta. A 55 (1999) 861-72.
17. F. Stenger, M. Gotzinger, P. Jakob, W. Peukert, Part. Part. Syst. Charact. 21 (2004) 31-38.
18. V. Srdic, L. Radonjic, J. Europ. Ceram. Soc., 14 (1994) 237-244.
19. J. Nyvt, O. Sohnel, M. Matuchova, M. Broul, in "The kinetics of industrial crystallization"(Elsevier, Amsterdam, 1985).
20. H. L. Wen, F. S.Yen, J. Crystal Growth, 208 [1-4] (2000) 696-708.
21. H. Zhang, J. F. Banfield, Chem. Mater., 14 (2002) 4145-54.
22. M. A. Stough, J. R. Hellmann Jr., J. Am. Ceram. Soc., 85 [12] (2002) 2895-902.
23. E. A. Pugar, P. E. D. Morgan, J. Am. Ceram. Soc., 69 [6] (1986) C120-123.